

## Research Article

# Pb(II) Removal Process in a Packed Column System with Xanthation-Modified Deoiled Allspice Husk

Efrain Palma-Anaya,<sup>1</sup> Cheikh Fall,<sup>2</sup> Teresa Torres-Blancas,<sup>1</sup> Patricia Balderas-Hernández,<sup>1</sup> Julian Cruz-Olivares,<sup>1</sup> Carlos E. Barrera-Díaz,<sup>1</sup> and Gabriela Roa-Morales<sup>1</sup>

<sup>1</sup>Centro Conjunto de Investigación en Química Sustentable (CCIQS), Universidad Autónoma del Estado de México (UAEMex), UAEM-UNAM, Carretera Toluca-Atacomulco, km 14.5, 50200 Toluca, MEX, Mexico

<sup>2</sup>Centro Interamericano de Recursos del Agua (CIRA), UAEMex, Carretera Toluca-Atacomulco, km 14.5, 50200 Toluca, MEX, Mexico

Correspondence should be addressed to Gabriela Roa-Morales; gabyroam@gmail.com

Received 24 July 2016; Revised 19 October 2016; Accepted 25 October 2016; Published 29 January 2017

Academic Editor: Julie J. M. Mesa

Copyright © 2017 Efrain Palma-Anaya et al. This is an open access article distributed under the Creative Commons Attribution License, which permits unrestricted use, distribution, and reproduction in any medium, provided the original work is properly cited.

The present research dealt with lead removal using modified *Pimenta dioica* L. Merrill as biosorbent in a batch and in continuous flow column systems, respectively. The allspice husk residues were modified first with a treatment through the xanthation reaction. For the adsorption tests, the atomic adsorption spectrophotometry method was used to determine the lead concentrations in the liquid samples. In the kinetic batch study (10 mg of sorbent in 10 mL of 25 mg L<sup>-1</sup> lead solution), the removal efficiency was 99% (adsorption capacity of 25.8 mg g<sup>-1</sup>). The kinetic data followed the pseudo-second-order model. The adsorption isotherm was fitted to the Freundlich model, where constants were  $K_f$  and  $1/n$  (8.06 mg<sup>(1-1/n)</sup> g<sup>-1</sup> L<sup>1/n</sup> and 0.52), corresponding to adsorption capacities of 8 and 62 mg g<sup>-1</sup>, at liquid equilibrium concentration of 1 and 50 mg L<sup>-1</sup>, respectively. In the continuous flow systems where lead solution of 50 mg L<sup>-1</sup> was treated in 2 columns of 5 cm (4.45 g) and 10 cm (9.07 g) bed heights, the dynamic adsorption capacity obtained by fitting the Thomas model was 29.114 mg g<sup>-1</sup> and 45.322 mg g<sup>-1</sup>, respectively.

## 1. Introduction

Needless to say, water is the main environmental constituent comprised on earth, as well as being the essential electrolyte for all living organisms in this planet [1]. The pollution of this unique resource has increased in recent years because of heavy metals discharges; therefore it is of great interest to devise methods to detect, quantify, and remove these metals [2]. The dangerousness of heavy metals is even greater, considering that they are not biodegradable and are persistent. Once emitted, they can remain in the atmosphere for hundreds of years. Lead in particular is a highly toxic metal that causes neurological damage to humans. The main way of transporting lead from intestines to any other tissues is through red blood cells, followed by absorption through blood, liver, and kidney. Because of its toxicity, lead inhibits the enzymatic action; that is, it can be fixed in blood, bones, and so on [3] because it displaces calcium since

they have similar atomic radius and because it has more affinity toward the functional groups present and produces alterations of the cell membrane [4, 5]. Recently, biosorption has been investigated as a very promising technology for the disposal of heavy metals especially in aqueous solution; it has the potential to do it efficiently, quickly, and at lower cost [6]. Therefore biosorption represents an alternative for conventional methods to dispose of metal ions. A broad range of biological materials, especially bacteria, algae, yeast, fungi, and agricultural industrial wastes, have received an increasing attention for the disposal of heavy metals, due to their good performance, low cost, and large quantities available [7, 8]. Previous studies indicate that biosorbents, in contrast to ion exchange functional resins, contain a variety of functional sites including imidazole, carboxyl, sulfhydryl, amino, phosphate, sulphate thioether, phenol, carbonyl, amide, and hydroxyl residues which allow us to obtain excellent results when using these materials [9, 10].

The development of new technologies for metal removal in aqueous solutions is convenient. This research work proposes a method of lead removal by biosorption as a conventional alternative to treat water polluted with this metal [11]. Chemical precipitation, oxidation, and ion exchange methods are expensive especially when the metal concentration is low; besides generation of sludge is high and its disposal becomes an environmental problem [12, 13].

In previous researches, the use of deoiled allspice husk residues for the Pb(II) removal in aqueous solution led to 78% removal in a batch system [14]. We have also used other biosorbents that were modified; for example, modified chitosan was used through a xanthation reaction to remove Pb(II) obtaining an 85% removal [15]. Another sort of biomass that can be used is orange peel, which likewise can be modified by a xanthation reaction, obtaining a Pb(II) removal of 95% [16]. Finally, residues chemically modified Lyocell for heavy metals treatment. The sorbent, which was prepared by a simple and concise method, was able to bind heavy metals such as Pb(II), Cu(II), and Cd(II), with very high efficiencies [17].

When doing chemical modifications to the used biosorbents, these increase their adsorption capacity because functional groups like amines, amides, thiols, imines, and phosphates become embedded. These create metal complexes or coordination complexes making the heavy metal adsorption process more efficient [18, 19]. The residues of *Pimenta dioica* L. Merrill, which belong to the Myrtaceae family, were used. Mexico exports about 4500 tons per year, and half of this production is processed domestically. In Mexico, 1500 tons of residues is produced annually as a result of the extraction of pepper essential oil. These residues contain 23.1% cellulose, 8.5% hemicellulose, and 26.8% lignin, among others. The pepper residues were modified by a xanthation reaction in a basic media, followed by a lead adsorption capacity test. Xanthation has been used before in pulp, sawdust, brown seaweed, and chitin; in every case an increase in the adsorption capacity was obtained [20]. Xanthates are created through the reaction of an organic substrate which contains hydroxyls with carbon disulphide; because of this, an increase of the biosorbent's affinity for Pb(II) is expected [21, 22].

## 2. Materials and Methods

**2.1. Biosorbent Previous Treatment.** 100 grammes of dry pepper residues with a particle size of 6 mm was vacuum-washed with 500 mL of a  $\text{H}_2\text{O}/\text{CH}_3\text{OH}$  (40%:60%) mix using a Buchner flask and a Buchner funnel. The pepper residues were dried for 24 h in a heater at  $70^\circ\text{C}$ . Then, a second vacuum wash was performed in the same conditions; then they were dried in a heater for 48 h, at  $70^\circ\text{C}$  [14].

**2.2. Modification of Pepper Residues by the Xanthation Reaction.** This amount of 100 gr of pepper residues already dried was added with 800 mL of NaOH 3 N (ACS Fermont 98.9%) and was left to react for 3 hours of stirring; after that, 50 mL of  $\text{CS}_2$  is added and left to react for 3 more hours [15]. Finally, we made a vacuum wash with deionized water to these pepper

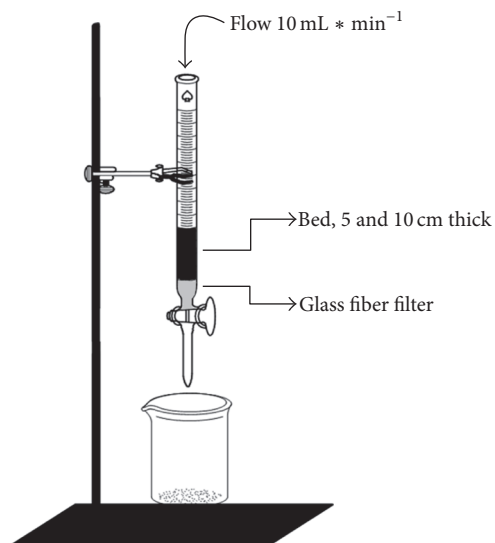


FIGURE 1: Column biosorbent with different thickness.

residues already modified which were let to dry at  $70^\circ\text{C}$  for 42 hours [21, 22].

**2.3. Pb(II) Solution Preparation.** A  $1000\text{ mg L}^{-1}$  lead stock solution was prepared, from which the following solutions were made: 0.05, 0.5, 1, 5, 10, 15, 20, 25, 30, 40, 50, 60, 70, and  $80\text{ mg L}^{-1}$ , setting the dissolutions pH to 4 with a  $0.001\text{ M}$  nitric acid solution.

**2.4. Adsorption in Batch System.** In order to study the adsorption kinetics of a  $10\text{ mL}$  lead solution of  $25\text{ mg L}^{-1}$  with a pH 4,  $10\text{ mg}$  of biosorbent was continuously shaken at  $30\text{ rpm}$ . The lead concentration in the system was established at 1, 5, 10, 15, 30, 45, 60, 75, 90, 105, and 120 minutes. To obtain the isotherms, solutions with different lead concentration levels were used that were 10, 20, 30, 40, and  $50\text{ mg L}^{-1}$  at pH 4 and then mixed with a  $10\text{ mg}$  biosorbent sample for 120 minutes at  $200\text{ rpm}$ . In both processes several tubes were prepared using the same method as the ones stated, but assigning each of them to a different contact time. Once the latter had elapsed, the residual lead concentrations were determined in their liquid phase using an atomic absorption spectrophotometer.

**2.5. Adsorption System in a Continuous Flow Column.** A  $40\text{ cm}$  length glass column with  $2\text{ cm}$  diameter was assembled. A fiberglass filter was assembled at the bottom to prevent any obstructions because of the biosorbent settling thereat. Each column was packed with pepper. Three tests with different biosorbent thicknesses were used (5 and  $10\text{ cm}$ ) using a burette clamp and a universal support, as shown in Figure 1.

A  $50\text{ mg L}^{-1}$  lead solution was passed through a packed column, by means of a fish tank pump and infusion instruments; the height was constantly regulated, just like the incoming and outgoing lead solution flow. Aliquots at the latter were gathered at different times; then, their lead

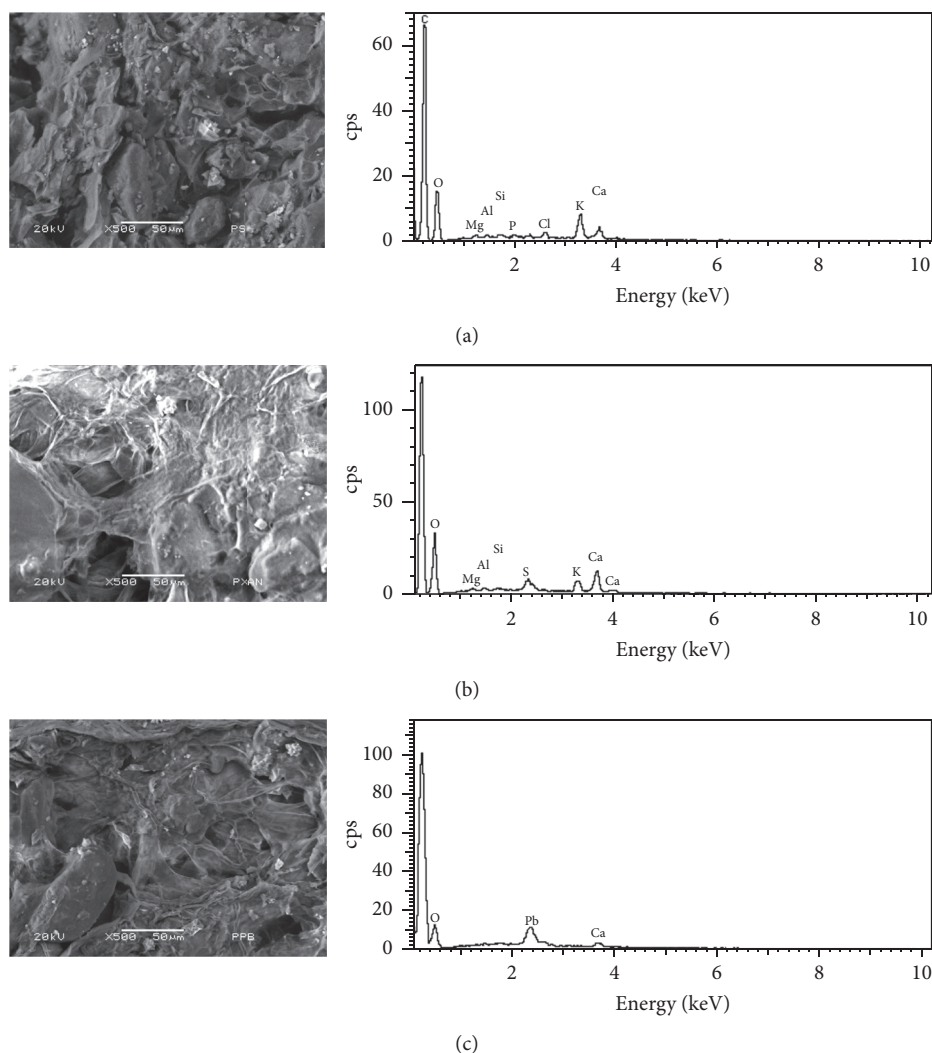


FIGURE 2: Micrographs pepper residues (a) unchanged, (b) modified, (c) after contact tests.

concentration was analyzed. This data was used to obtain the breakthrough curves.

## 2.6. Material Characterization

**2.6.1. BET Analysis.** The surface area and characteristics of the modified and unmodified pepper porosity were determined by means of  $N_2$  BET gas method (GEMINI 2360 equipment) adsorbing nitrogen at 77 K. The respective adsorption isotherms were then recorded until attaining a 0.9 relative pressure in order to estimate the overall porosity volume: the porosity was determined using their volume and density.

**2.6.2. Scanning Electron Microscope.** The biosorbent images were obtained with a JEOL JSM 6510LV to 15 kV with 10 mm WD. The samples were covered with a 20  $\mu\text{m}$  gold layer by means of sputtering with a Denton Vacuum DESK IV gold objective.

**2.6.3. Infrared Spectroscopy.** In order to identify the main functional groups involved in each process, the Fourier transform infrared (FTIR) spectroscopy was used, thus recording the infrared spectrum of the modified and unmodified pepper before and after the adsorption test in the batch system.

## 3. Results and Discussion

### 3.1. Biosorbent Characterization

**3.1.1. MEB (SEM) Test.** Figure 2 shows the MEB secondary electron images of pepper residues before modifying through the xanthation reaction, after the modification and after the adsorption test. Figure 2(a) shows the morphology of original material, comprising amorphous and irregular structures, though showing above all a large number of pores, with 50  $\mu\text{m}$  length approximate particle size. The energy dispersion analysis gives the elemental composition of the

TABLE I: Results of surface area.

	Specific surface area	Mean pore diameter
Unmodified pepper	$1.65 \text{ m}^2 \cdot \text{g}^{-1}$	5.71 nm
Modified pepper	$1.72 \text{ m}^2 \cdot \text{g}^{-1}$	3.02 nm

pepper residues, comprising at large carbon and oxygen, approximately representing 64.9% and 32.9%, respectively, of the total weight; small Mg, Al, Si, P, Cl, K, and Ca quantities are included. Figure 2(b) shows the pepper residues image after the xanthation modification. An amorphous and porous structure is visible, a particle size of  $50 \mu\text{m}$  length in the magnified micrograph of 500x. For the elemental composition of the pepper residues after the modification through xanthation the majority elements are carbon and oxygen with the 60.509% and 36.817%, respectively, although sulphur is now present, which was expected because this group increases after modification. Figure 2(c) shows the image of the pepper residues already modified; after doing the adsorption tests, the resulting structure is amorphous and porous similar to the previous images: also, the particle size was  $50 \mu\text{m}$ .

The elemental composition of the pepper residues after contact with the Pb(II) solution revealed that carbon and oxygen seem to be the majority with 67.636% and 28.642%, respectively, but now Pb(II) is present, which was expected though not in a higher percentage, because the particle size that was used was too large; thus there is a higher quantity of pores but there is also a smaller quantity of Ca.

**3.1.2. BET Analysis.** In Table 1 it is disclosed that the surface area of the biosorbent is  $1.72 \text{ m}^2 \cdot \text{g}^{-1}$  which is lower than that of the activated carbon with  $500\text{--}1500 \text{ m}^2 \cdot \text{g}^{-1}$ , but that does not limit its adsorption capacity. Doing the modification did not increase considerably the material attributes [23].

**3.1.3. Infrared Spectroscopy.** Figure 3 shows the IR spectra that were obtained from the pepper residues before they were modified and after the contact tests, where the most important functional groups of each process are located and detailed. A characteristic -OH band was located at the  $3000 \text{ cm}^{-1}$  that reflects bond stretching; another band that was located at  $1600 \text{ cm}^{-1}$  comes from carbonyl vibration associated with the essential oil traces and the band located between  $1300 \text{ cm}^{-1}$  and  $1500 \text{ cm}^{-1}$  comes from the stretching vibrations of a C-O interaction associated with primary and secondary alcohols that are dissociated.

The band at  $1100 \text{ cm}^{-1}$  is due to the vibration between the C=S interaction and the band that at  $1050 \text{ cm}^{-1}$  is due to sulfoxides functional group C-S or O-C-S vibration, which demonstrate that the pepper modification was done, since the presence of S is observed.

**3.2. Distribution Diagram of Lead Species.** It has been stated that all tests of this study were made at pH 4, because the distribution diagram of the lead species shown in Figure 4 showed that any pH above 6 would involve lead precipitation;

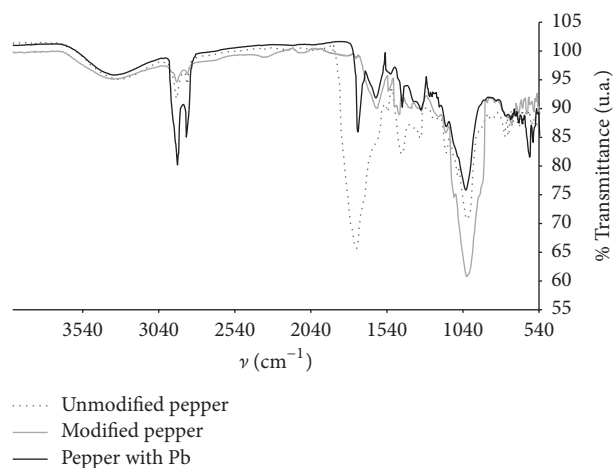


FIGURE 3: IR pepper residue unmodified and modified after contact tests.

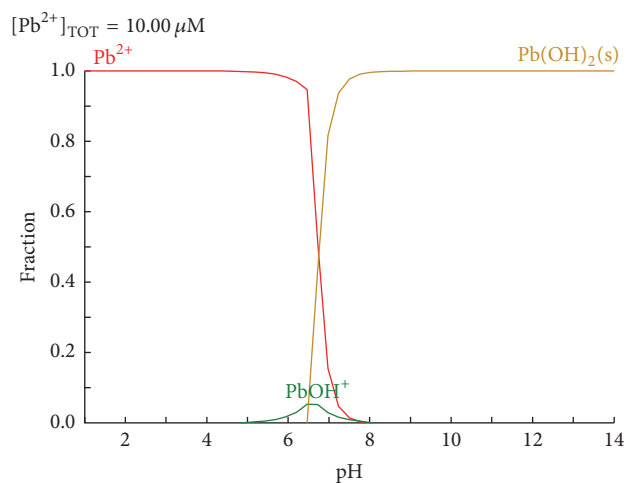


FIGURE 4: Diagram of distribution of lead species [I. Puigdomenech, Hydrochemical Equilibrium Constants Database (MEDUSA), Royal Institute of Technology, Stockholm, Sweden, 1997].

therefore the removal would not be through adsorption. Working in the  $\text{pH} < 6$  zone would warrant that lead remained as  $\text{Pb}^{2+}$ . However, working with a  $\text{pH}$  3 or smaller, a precipitation problem would not occur, although the working conditions would not be appropriate, considering that an acidic media prevailed, where the  $\text{Pb}^{2+}$  species would have to compete with  $\text{H}^+$  for the biosorbent active place, thereby causing a protonation process of the biosorbent, affecting the lead removal process again [24, 25].

**3.3. Batch Adsorption Kinetics.** These tests were made with a  $25 \text{ mg L}^{-1}$  lead solution at  $\text{pH}$  4 with constant stirring at 200 rpm and 10 mg of biosorbent. As shown in Figure 5, during the first 10 contact minutes, the concentration of Pb(II) in solution decreased almost to one-half, obtaining the acutest Pb(II) decrease during the first 5 minutes. Then, the Pb(II) concentration in solution decreased with increasing stirring time until reaching a quasi-equilibrium.

TABLE 2: Parameters from the pseudo-second-order kinetic model.

$C_o$ (mg·L <sup>-1</sup> )	$q_2$ (mg·g <sup>-1</sup> )	$q_{exp}$ (mg·g <sup>-1</sup> )	$K_2$ (g·mg <sup>-1</sup> min <sup>-1</sup> )	$R^2$
25	27.03	25.8	$4.67 \times 10^{-3}$	0.993

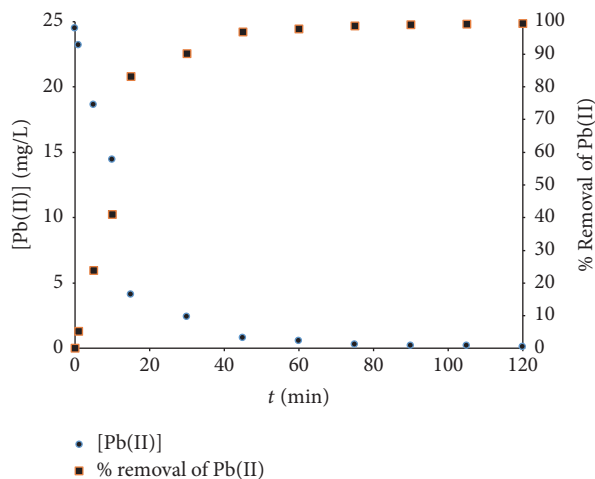


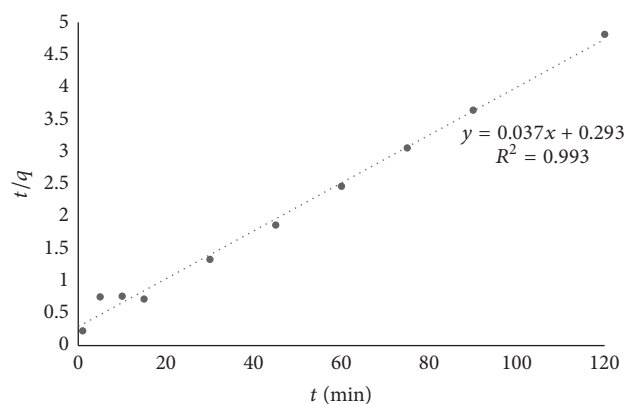
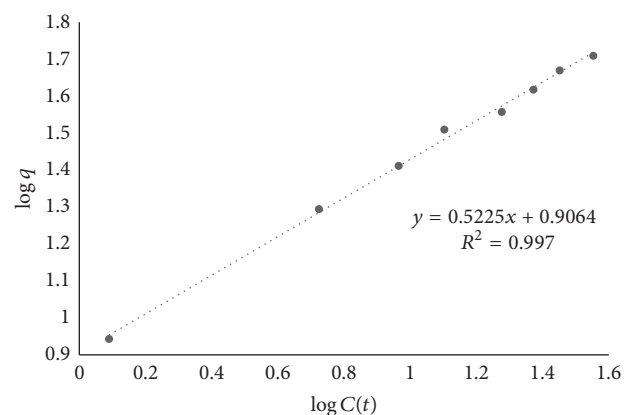
FIGURE 5: Concentration and lead removal percentage versus time at a pH value of 4 for the system Pb(II) and pepper modified with a particle size of 6 mm.

Figure 5 shows the removal percentage achieved after 120 contact minutes, reaching the 99%, which was very good, therefore confirming the efficiency of the modified biosorbent. The kinetic model with the best fitting was the pseudo-second-order model, with a correlation coefficient  $R^2 = 0.99$ , shown in Figure 6. The adsorption process kinetic was described by

$$\frac{1}{q_t} = \frac{1}{k_2 q_2^2} + \frac{1}{q_2} t, \quad (1)$$

where  $q_2$  is the equilibrium adsorption capacity (mg g<sup>-1</sup>) predicted by the pseudo-second-order (for a  $C_o = 25$  mg L<sup>-1</sup>) adsorption when the initial  $q_t$  is the quantity of adsorbed metal at the time  $t$  (mg g<sup>-1</sup>) and  $K_2$  is the pseudo-second-order speed constant (mg g<sup>-1</sup> min<sup>-1</sup>) [26, 27]. Table 2 indicated that calculated  $q_2$  is 27.03 mg g<sup>-1</sup>, while  $K_2$  was  $4.67 \times 10^{-3}$  g mg<sup>-1</sup> min<sup>-1</sup>. The  $q_2$  value was estimated through mass balance with the last data of concentration in the liquid at 120 minutes giving a  $q_{exp}$  value of 25.8, which is comparable to the  $q_2$  value obtained in the kinetic model [28, 29].

These results are similar to those obtained by [14] because in the previous study it was made with xanthated pepper with a particle size of 2.36 mm where they obtained a kinetic adsorption of pseudo-second order with a  $K_2$  of 7.46 g mg<sup>-1</sup> min<sup>-1</sup> and a  $q_2$  of 38.74 mg g<sup>-1</sup>, which are values slightly higher than those obtained in this study but that agree with the particle size used in both studies. Based on the results shown, the studies to obtain the adsorption isotherm using different Pb(II) concentrations were made.

FIGURE 6: Kinetics of adsorption of pseudo-second-order  $q/t$  versus time, for the system of Pb(II) and pepper modified with a particle size of 6 mm.FIGURE 7:  $\log q$  Freundlich isotherm according to the system  $\log C(t)$  of Pb(II) and pepper modified with a particle size of 6 mm.

**3.3.1. Adsorption Isotherm.** Figure 7 shows that the Freundlich isotherm model fitted well the data, giving a correlation coefficient  $R^2 = 0.997$ . The Freundlich isotherm fits well into the experimental data; consequently multilayer adsorption with heterogeneous distribution of active sites of the biosorbent is proposed [30, 31].

The values for Freundlich isotherm constants were  $K_f = 8.06$  (mg g<sup>-1</sup>) (mg<sup>-1/n</sup> L<sup>1/n</sup>) and  $1/n = 0.52$ , respectively [32, 33].

**3.4. Continuous Flow Column System.** Figure 8 shows the breakthrough curves that were obtained working with biosorbent beds of 5 cm and 10 cm height, with a flow of 10 mL min<sup>-1</sup> and with a lead solution of 50 mg L<sup>-1</sup>. With the

TABLE 3: Parameters of the Thomas model for the bed heights of 5 cm and 10 cm.

Bed height (cm)	Biosorbent used (g)	Flow of the Pb(II) solution (mL·min <sup>-1</sup> )	$K_{TH}$ (L·min <sup>-1</sup> ·mg <sup>-1</sup> )	$q_o$ (mg·g <sup>-1</sup> )	$r^2$
10	9.07	10	0.0026	45.322	0.98
5	4.45	10	0.0035	29.114	0.98

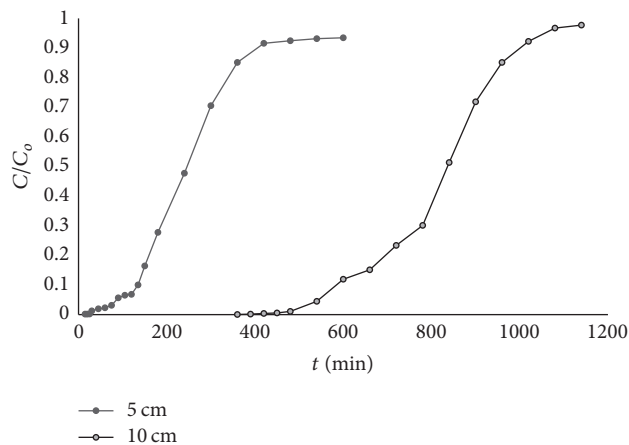


FIGURE 8: Breakthrough curves of the 5 and 10 cm columns packed with modified pepper (6 mm particle size).

10 cm height bed, 90% saturation occurs after 1000 minutes of operating time, although a complete saturation was not seen during the follow-up time.

Working with a biosorbent bed, 5 cm thick, saturation occurred after 300 minutes of operating time. The data obtained were analyzed mathematically using the Thomas model. The successful design of a sorption process in a column requires the prediction of the breakthrough curve for the effluent and the specification of the maximum sorption capacity of the sorbent. The linearized form of the equations is presented by the following Thomas equation:

$$\ln\left(\frac{C_o}{C} - 1\right) = \frac{K_{TH}q_oM}{Q} - K_{TH}C_o t, \quad (2)$$

where  $C$  is solute concentration in the affluent (mg·L<sup>-1</sup>),  $C_o$  is solute concentration in the influent (mg·L<sup>-1</sup>),  $K$  is Thomas speed constant (mg min<sup>-1</sup> mg<sup>-1</sup>),  $q_o$  is maximum concentration of solute in the solid phase (mg g<sup>-1</sup>),  $M$  is mass of sorbent (g),  $t$  is time (min), and  $Q$  is volumetric flow rate (mL min<sup>-1</sup>).

Table 3 shows the results from the fitting of the Thomas model [33, 34]. By working with a xanthated pepper bed, 5 cm thick, a maximum adsorption capacity of 29.114 mg g<sup>-1</sup> was obtained with a rate constant of 0.0035 L min<sup>-1</sup> mg<sup>-1</sup>, with a coefficient of determination ( $r^2$ ) of 0.98, which is shown in Figure 9. With 10 cm bed, the maximum adsorption capacity was 45.322 mg g<sup>-1</sup> while the Thomas kinetic constant was 0.0026 L min<sup>-1</sup> mg<sup>-1</sup> ( $r^2 = 0.98$ , also shown in Figure 9).

#### 4. Conclusions

The removal percentage of Pb(II) in aqueous solution obtained was 99% at pH 4; the Pb(II) removal in aqueous

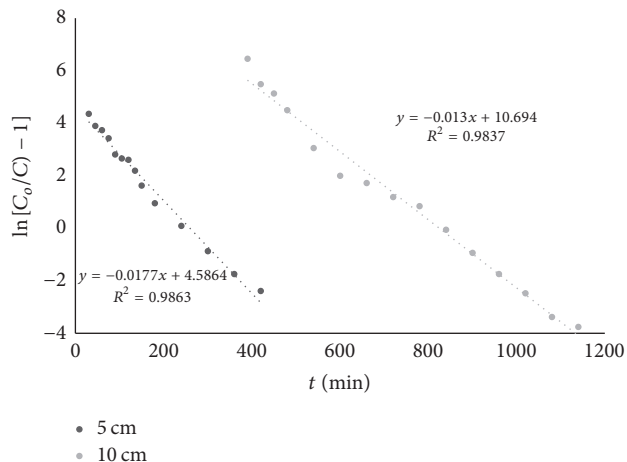


FIGURE 9: Fitting of the linearized Thomas model with data from the packed column of 5 and 10 cm (modified pepper adsorbent of 6 mm particle size).

solution was favoured by the modification done to the pepper residues, which increased the biosorbent affinity for Pb(II). The results from the batch kinetic studies showed a maximum adsorption capacity of 25.8 mg of Pb(II) per g of biosorbent, while the data were well fitted by the pseudo-second-order kinetic model. Pb(II) in aqueous solution was adsorbed through a multilayer process with heterogeneous distribution of the biosorbent's active sites. The infrared and scanning electron microscope studies verified that the sulphur insertion created the thiol group in the pepper structure, which was the aim of the biosorbent modification. The breakthrough curves of the continuous flow systems (columns) were adequately fitted with the Thomas model, which provided an estimation of the dynamic adsorption capacities of 29.114 mg g<sup>-1</sup> and 45.322 mg g<sup>-1</sup> (for the 5 and 10 cm bed height, resp.).

#### Competing Interests

The authors declare that they have no competing interests.

#### Acknowledgments

Efrain Palma-Anaya gratefully acknowledges the scholarship from CONACyT to pursue her postgraduate studies.

#### References

- [1] T. H. Bakken, I. S. Modahl, K. Engeland, H. L. Raadal, and S. Arnøy, "The life-cycle water footprint of two hydropower projects in Norway," *Journal of Cleaner Production*, vol. 113, pp. 241–250, 2016.

- [2] S. Chowdhury, M. A. J. Mazumder, O. Al-Attas, and T. Husain, "Heavy metals in drinking water: occurrences, implications, and future needs in developing countries," *Science of the Total Environment*, vol. 569–570, pp. 476–488, 2016.
- [3] V. Geraldes, M. Carvalho, N. Goncalves-Rosa, C. Tavares, S. Laranjo, and I. Rocha, "Lead toxicity promotes autonomic dysfunction with increased chemoreceptor sensitivity," *Neuro-Toxicology*, vol. 54, pp. 170–177, 2016.
- [4] M. Dörpinghaus, A. Brieger, O. Panichkina, L. Rink, and H. Haase, "Lead ions abrogate lipopolysaccharide-induced nitric monoxide toxicity by reducing the expression of STAT1 and iNOS," *Journal of Trace Elements in Medicine and Biology*, vol. 37, pp. 117–124, 2016.
- [5] C. M. V. B. Almeida, M. A. Madureira, S. H. Bonilla, and B. F. Giannetti, "Assessing the replacement of lead in solders: effects on resource use and human health," *Journal of Cleaner Production*, vol. 47, pp. 457–464, 2013.
- [6] H. T. Tran, N. D. Vu, M. Matsukawa et al., "Heavy metal biosorption from aqueous solutions by algae inhabiting rice paddies in Vietnam," *Journal of Environmental Chemical Engineering*, vol. 4, no. 2, pp. 2529–2535, 2016.
- [7] A. K. Zeraatkar, H. Ahmadzadeh, A. F. Talebi, N. R. Moheimani, and M. P. McHenry, "Potential use of algae for heavy metal bioremediation, a critical review," *Journal of Environmental Management*, vol. 181, no. 1, pp. 817–831, 2016.
- [8] J. Milojković, L. Pezo, M. Stojanović et al., "Selected heavy metal biosorption by compost of *Myriophyllum spicatum*—a chemometric approach," *Ecological Engineering*, vol. 93, pp. 112–119, 2016.
- [9] N. K. Akunwa, M. N. Muhammad, and J. C. Akunna, "Treatment of metal-contaminated wastewater: a comparison of low-cost biosorbents," *Journal of Environmental Management*, vol. 146, pp. 517–523, 2014.
- [10] R. K. Gautam, A. Mudhoo, G. Lofrano, and M. C. Chattopadhyaya, "Biomass-derived biosorbents for metal ions sequestration: adsorbent modification and activation methods and adsorbent regeneration," *Journal of Environmental Chemical Engineering*, vol. 2, no. 1, pp. 239–259, 2014.
- [11] K. M. Al-Qahtani, "Water purification using different waste fruit cortexes for the removal of heavy metals," *Journal of Taibah University for Science*, vol. 10, no. 5, pp. 700–708, 2016.
- [12] J. Zhao, J. Liu, N. Li et al., "Highly efficient removal of bivalent heavy metals from aqueous systems by magnetic porous  $\text{Fe}_3\text{O}_4$ - $\text{MnO}_2$ : adsorption behavior and process study," *Chemical Engineering Journal*, vol. 304, pp. 737–746, 2016.
- [13] J. Mehta, S. K. Bhardwaj, N. Bhardwaj et al., "Progress in the biosensing techniques for trace-level heavy metals," *Biotechnology Advances*, vol. 34, no. 1, pp. 47–60, 2016.
- [14] T. Torres-Blancas, G. Roa-Morales, C. Fall, C. Barrera-Díaz, F. Ureña-Núñez, and T. B. Pavón Silva, "Improving lead sorption through chemical modification of de-oiled allspice husk by xanthate," *Fuel*, vol. 110, pp. 4–11, 2013.
- [15] D. Chauhan and N. Sankaramakrishnan, "Highly enhanced adsorption for decontamination of lead ions from battery wastewaters using chitosan functionalized with xanthate," *Bioresource Technology*, vol. 99, no. 18, pp. 9021–9024, 2008.
- [16] N.-C. Feng and X.-Y. Guo, "Characterization of adsorptive capacity and mechanisms on adsorption of copper, lead and zinc by modified orange peel," *Transactions of Nonferrous Metals Society of China*, vol. 22, no. 5, pp. 1224–1231, 2012.
- [17] J. K. Bediako, W. Wei, S. Kim, and Y.-S. Yun, "Removal of heavy metals from aqueous phases using chemically modified waste Lyocell fiber," *Journal of Hazardous Materials*, vol. 299, pp. 550–561, 2015.
- [18] U. Farooq Umar, M. A. Khan, M. Athar, and J. A. Kozinski, "Effect of modification of environmentally friendly biosorbent wheat (*Triticum aestivum*) on the biosorptive removal of cadmium(II) ions from aqueous solution," *Chemical Engineering Journal*, vol. 171, no. 2, pp. 400–410, 2011.
- [19] S. W. Won, P. Kotte, W. Wei, A. Lim, and Y.-S. Yun, "Biosorbents for recovery of precious metals," *Bioresource Technology*, vol. 160, pp. 203–212, 2014.
- [20] K. Wang, L. Wang, M. Cao, and Q. Liu, "Xanthation-modified polyacrylamide and spectroscopic investigation of its adsorption onto mineral surfaces," *Minerals Engineering*, vol. 39, pp. 1–8, 2012.
- [21] S. Liang, X. Guo, N. Feng, and Q. Tian, "Application of orange peel xanthate for the adsorption of  $\text{Pb}^{2+}$  from aqueous solutions," *Journal of Hazardous Materials*, vol. 170, no. 1, pp. 425–429, 2009.
- [22] P. L. Homagai, K. N. Ghimire, and K. Inoue, "Adsorption behavior of heavy metals onto chemically modified sugarcane bagasse," *Bioresource Technology*, vol. 101, no. 6, pp. 2067–2069, 2010.
- [23] M. T. Izquierdo, A. M. De Yuso, R. Valenciano, B. Rubio, and M. R. Pino, "Influence of activated carbon characteristics on toluene and hexane adsorption: application of surface response methodology," *Applied Surface Science*, vol. 264, pp. 335–343, 2013.
- [24] A. Hammami, F. González, A. Ballester, M. L. Blázquez, and J. A. Muñoz, "Biosorption of heavy metals by activated sludge and their desorption characteristics," *Journal of Environmental Management*, vol. 84, no. 4, pp. 419–426, 2007.
- [25] B. F. Trueman and G. A. Gagnon, "A new analytical approach to understanding nanoscale lead-iron interactions in drinking water distribution systems," *Journal of Hazardous Materials*, vol. 311, pp. 151–157, 2016.
- [26] L. Largette and R. Pasquier, "A review of the kinetics adsorption models and their application to the adsorption of lead by an activated carbon," *Chemical Engineering Research and Design*, vol. 109, pp. 495–504, 2016.
- [27] R. K. Anantha and S. Kota, "Removal of lead by adsorption with the renewable biopolymer composite of feather (*Dromaius novaehollandiae*) and chitosan (*Agaricus bisporus*)," *Environmental Technology and Innovation*, vol. 6, pp. 11–26, 2016.
- [28] L. Largette and R. Pasquier, "New models for kinetics and equilibrium homogeneous adsorption," *Chemical Engineering Research and Design*, vol. 112, pp. 289–297, 2016.
- [29] M. M. Montazer-Rahmati, P. Rabbani, A. Abdolali, and A. R. Keshtkar, "Kinetics and equilibrium studies on biosorption of cadmium, lead, and nickel ions from aqueous solutions by intact and chemically modified brown algae," *Journal of Hazardous Materials*, vol. 185, no. 1, pp. 401–407, 2011.
- [30] Y. P. Teoh, M. A. Khan, and T. S. Y. Choong, "Kinetic and isotherm studies for lead adsorption from aqueous phase on carbon coated monolith," *Chemical Engineering Journal*, vol. 217, pp. 248–255, 2013.
- [31] S. Tunali Akar, S. Arslan, T. Alp, D. Arslan, and T. Akar, "Biosorption potential of the waste biomaterial obtained from Cucumis melo for the removal of  $\text{Pb}^{2+}$  ions from aqueous media: equilibrium, kinetic, thermodynamic and mechanism analysis," *Chemical Engineering Journal*, vol. 185–186, pp. 82–90, 2012.

- [32] D. Bulgariu and L. Bulgariu, "Equilibrium and kinetics studies of heavy metal ions biosorption on green algae waste biomass," *Bioresource Technology*, vol. 103, no. 1, pp. 489–493, 2012.
- [33] Q. Li, H. Lu, H. Xiao, K. Gao, and M. Diao, "Adsorption capacity of superabsorbent resin composite enhanced by non-thermal plasma and its adsorption kinetics and isotherms to lead ion in water," *Journal of Environmental Chemical Engineering*, vol. 1, no. 4, pp. 996–1003, 2013.
- [34] S. Amirnia, M. B. Ray, and A. Margaritis, "Heavy metals removal from aqueous solutions using *Saccharomyces cerevisiae* in a novel continuous bioreactor–biosorption system," *Chemical Engineering Journal*, vol. 264, pp. 863–872, 2015.

